Supplementary Information

Polymer architecture as key to unprecedented high-resolution 3D-printing performance: The case of biodegradable hexa-functional telechelic urethane-based poly-ε-caprolactone

Aysu Arslan[1,a], Wolfgang Steiger[2,3,a], Patrice Roose[4], Hugues Van den Bergen[4], Peter Gruber[2,3], Elise Zerobin[3,5], Franziska Gantner[2,3], Olivier Guillaume[2,3], Aleksandr Ovsianikov[2,3,b], Sandra Van Vlierberghe[1,6,c], Peter Dubruel[1,c]

[1] Polymer Chemistry & Biomaterials Research Group, Centre of Macromolecular Chemistry (CMaC), Ghent University, Krijgslaan 281 S4-Bis, 9000 Ghent, Belgium

[2] 3D Printing and Biofabrication Group, Institute of Materials Science and Technology, TU Wien, 1060 Vienna, Austria

[3] Austrian Cluster for Tissue Regeneration (http://www.tissue-regeneration.at)

[4] allnex Belgium SA/NV, Anderlechtstraat 33, Drogenbos, Belgium

[5] Institute of Applied Synthetic Chemistry, TU Wien, 1060 Vienna, Austria

[6] Brussels Photonics, Department of Applied Physics and Photonics, Vrije Universiteit Brussel, Pleinlaan 2, 1050 Elsene, Belgium

[a] Equally contributed first authors.

[b] Corresponding author. *E-mail address: Ovsianikov, A. (aleksandr.ovsianikov@tuwien.ac.at)*

[c] Equally contributed last authors.

1. Synthesis of the precursors

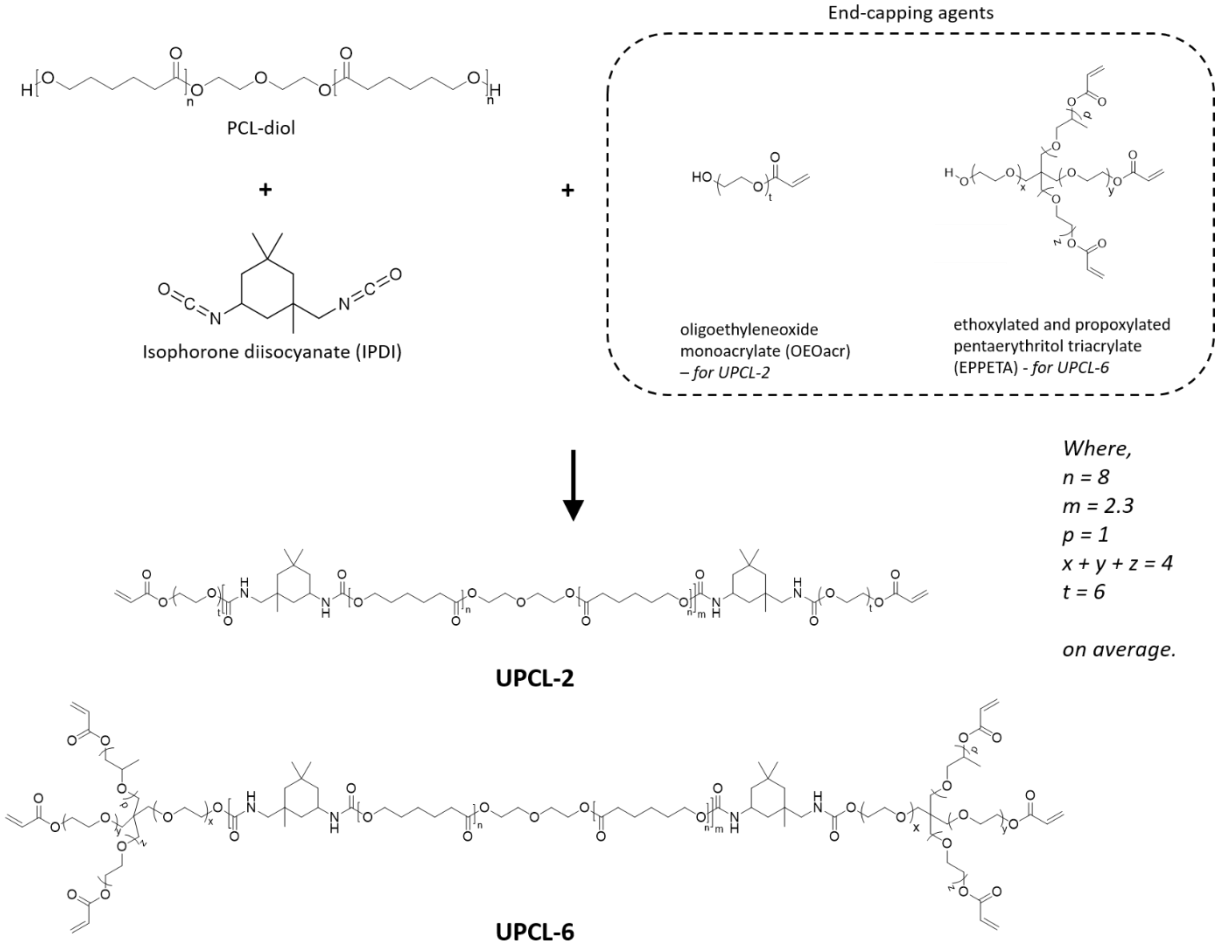

S1*: *Chemical structures of the reagents and the final products

2. Nuclear magnetic resonance (^{1}H-NMR) spectroscopy

The precursors were analyzed via ^{1}H-NMR spectroscopy (Bruker Avance 400 MHz Spectrometer). The precursors were dissolved in deuterated chloroform ($CDCl_3$, Euriso-Top) prior to analysis. For the calculation of the acrylate concentrations, dimethyl terephthalate (DMT, Sigma Aldrich) was used as standard. Both precursors and DMT were weighed using an analytical balance and dissolved together in $CDCl_3$ prior to analysis. The spectra were analyzed using the MestReNova software (version 6.0.2). The amount of acrylates present in the precursors was calculated using the equation below.

$$C_{acr} = \frac{I_{\delta=5.8ppm} + I_{\delta=6.1ppm} + I_{\delta=6.3ppm}}{I_{\delta=8ppm}} \times \frac{N_{H,\delta=8ppm}}{N_{\delta=5.8ppm} + N_{\delta=6.1ppm} + N_{\delta=6.3ppm}} \times \frac{W_{DMT}}{MW_{DMT}} \times \frac{1000}{W_p}$$

(Equation S1)

where C_{acr} is the amount of acrylates in the precursors (mmol acrylate/g precursor), ($I_{\delta=5.8ppm} + I_{\delta=6.1ppm} + I_{\delta=6.3ppm}$) is the sum of the integrals of the signals of the protons arising from the acrylates (*δ=5.83, 6.12 and 6.40 ppm),* $I_{\delta=8ppm}$ is the integral of the signal of the protons characteristic for the aromatic ring in DMT (*δ=8ppm), (*$N_{\delta=5.8ppm} + N_{\delta=6.1ppm} + N_{\delta=6.3ppm}$) is the number of protons in one acrylate end group, $N_{H,\ \delta=8ppm}$ is the number of protons in the benzene ring of DMT, W_{DMT} is the weight of DMT (g), W_p is the weight of precursor (g) and MW_{DMT} is the molar mass of DMT (g mol^{-1}).

Theoretical acrylate concentrations in the final product were estimated according to the equation below:

$$C_{acr}^{th} = (C_{acr}^{ECA} \times W_{ECA}) / (W_{PCL} + W_{IPDI} + W_{ECA}) \quad \textbf{(Equation S2)}$$

Where C_{acr}^{th} is the theoretical acrylate concentration (mmol acrylate/g precursor), C_{acr}^{ECA} is the acrylate concentration in the end-capping agent (mmol acrylate, g ECA, determined experimentally via ^{1}H-NMR), W_{PCL}, W_{IPDI} and W_{ECA} are the weights (g) of reagents PCLdiol, IPDI and end-capping agents used in the reactions, respectively.

The acrylate concentrations (C_{acr}) determined experimentally using Eq. S1 and theoretical acrylate concentrations (C_{acr}^{th}) calculated using eq. S2 were presented in table below.

	C_{acr} (mmol g^{-1})	C_{acr}^{ECA} (mmol g^{-1})	W_{ECA} (g)	W_{PCL} (g)	W_{IPDI} (g)	C_{acr}^{th} (mmol g^{-1})
UPCL-2	0.60	2.66	20.2	60	13.3	0.57
UPCL-6	1.74	5.46	34.3	60	13.3	1.74

The acrylate concentrations of UPCL-2 (0.60 mmol g^{-1})and UPCL-6 (1.74 mmol g^{-1}) that were experimentally determined via ^{1}H-NMR spectroscopy (Eq. S1) were in excellent agreement with theoretical acrylate concentrations (0.57 and 1.74 mmol g^{-1} for UPCL-2 and UPCL-6, respectively) (Eq. S2), indicating that the acrylate groups remained stable throughout the reaction.

In the ^{1}H-NMR spectrum (Figure S2), the signals around δ=4.0, δ=2.3 and δ=1.5 ppm correspond to the CH_2 protons from the ε-caprolactone units. The signals between δ=3.3 and δ=3.8 ppm can be attributed to the methylene protons present in the ethylene oxide spacers (and the propylene oxide spacers in case of UPCL-6). The protons in the methylene groups of alkoxy spacer groups that are adjacent to urethane groups and acrylate esters can be seen at δ=4.15 and δ=4.25 ppm, respectively. The signals between δ=0.7 and δ=1.3 ppm correspond to the protons from the methylene units in the cyclic IPDI and the signals at δ=6.3, δ=6.1 and δ=5.8 ppm arise from the acrylate protons in the final products.

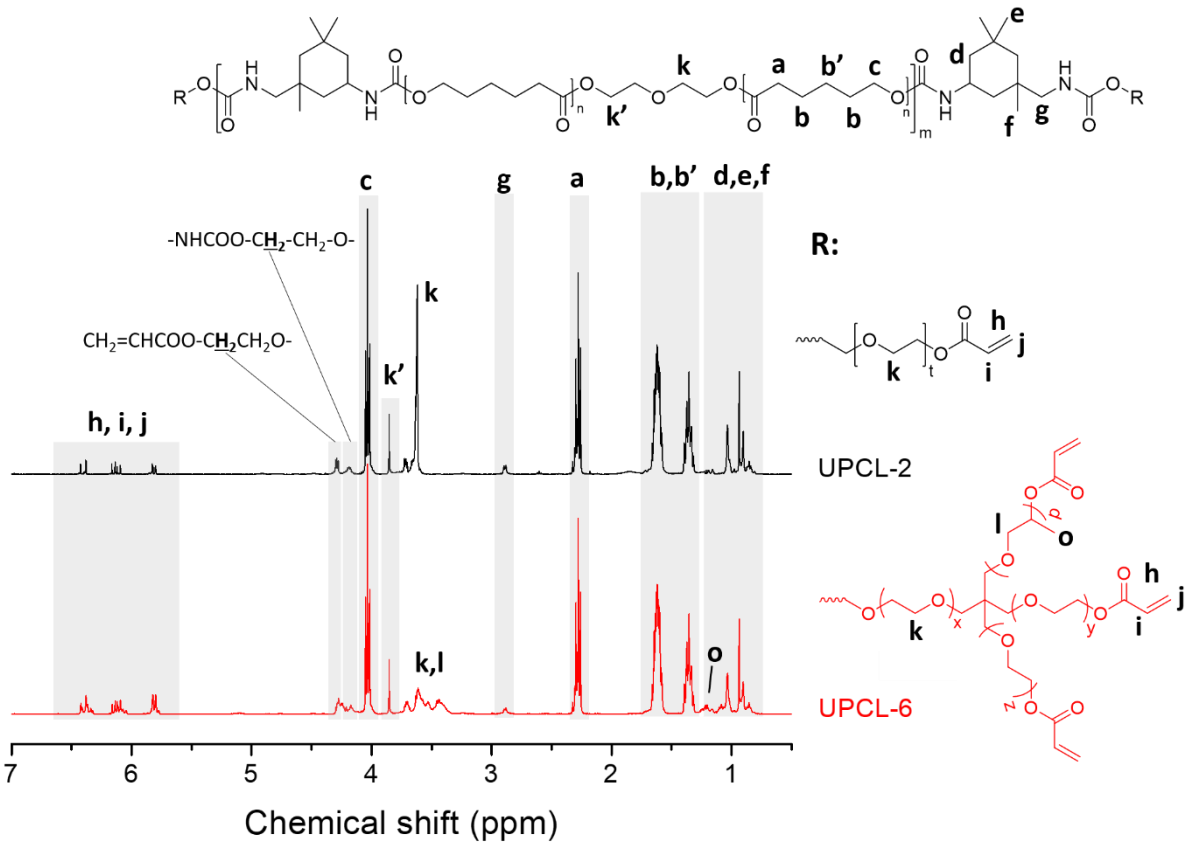

S2: *^{1}H-NMR spectra and the chemical structures of UPCL-2 and UPCL-6*

3. Fourier transform infrared spectroscopy

FTIR spectroscopy was performed on a FTIR spectrometer (Perkin Elmer) operating in Attenuated Total Reflection (ATR) mode. Spectra of the starting polymer PCL-diol, the intermediate product obtained after the first step of the reaction (PCL-IPDI) and the final products were recorded in the range of 600–4000 cm^{-1} using 8 scans.

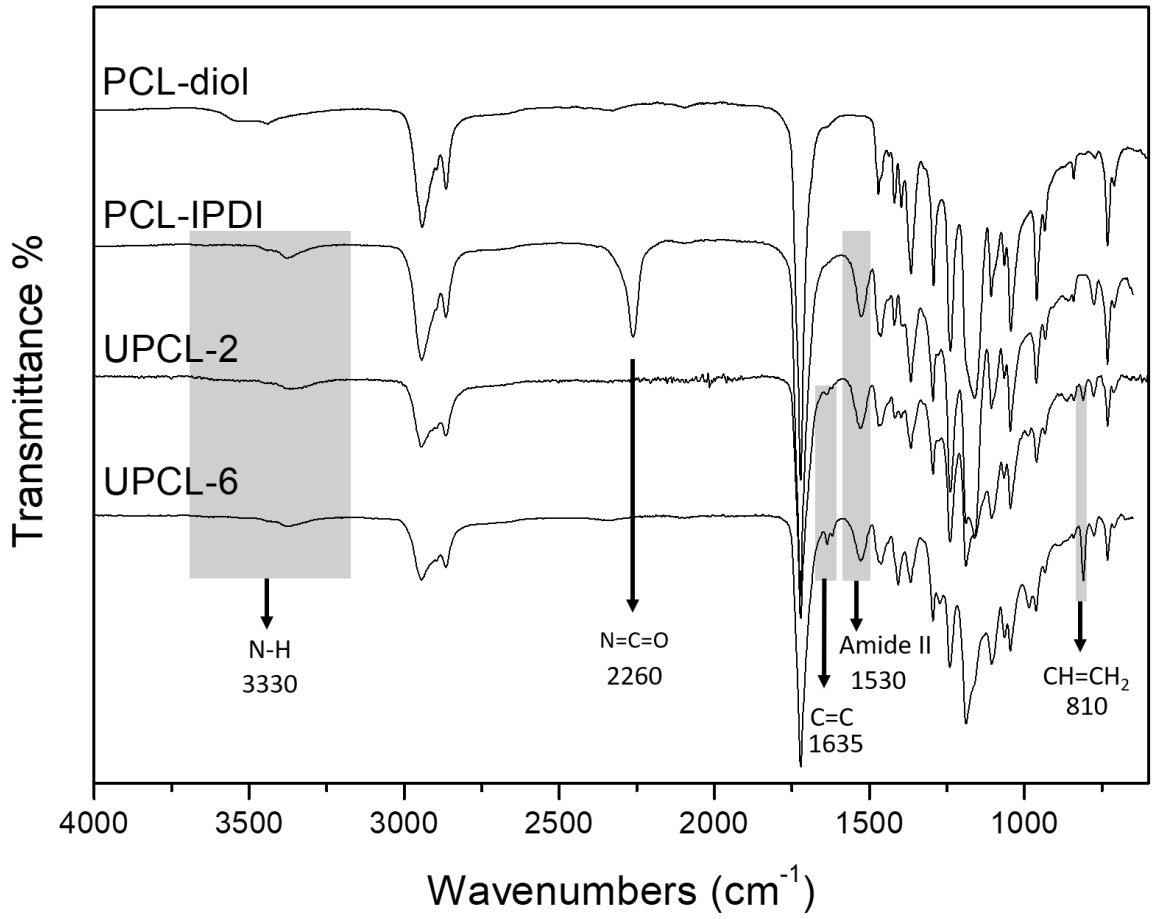

S3: *FTIR spectra of the starting polymer (PCL-diol), the intermediate product resulting from the 1st reaction step (PCL-IPDI) and the final products UPCL-2 and UPCL-6.*

The FTIR spectrum of PCL-IPDI reveals the characteristic absorption bands corresponding to the N-H stretching (3330 cm^{-1}) and amide II (1530 cm^{-1}) confirming the urethanization reaction proceeded in the 1st reaction step. The spectra of the final products UPCL-2 and UPCL-6 confirm the complete conversion of the isocyanate groups reacting with the hydroxyl moieties of PCL-diol and those of the end-capping agents, as the characteristic absorption band corresponding to the free isocyanate groups (2260 cm^{-1}) disappeared after the 2nd reaction step. The absorption bands at 1635 cm^{-1} and 810 cm^{-1} corresponding to the C=C stretch and the =C-H_2 out-of-plane deformation of the acrylate groups can be observed in the spectra of the final products.

4. Gel permeation chromatography

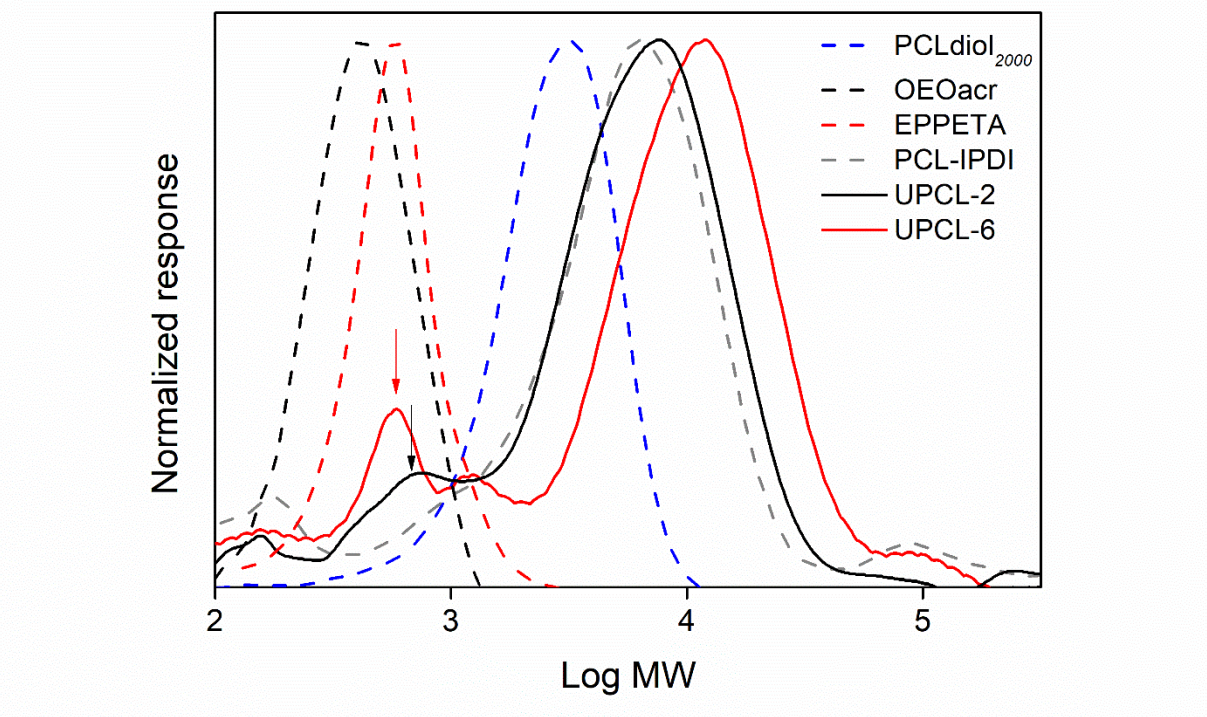

S4: *GPC chromatogram of unmodified PCLdiol (2000 g/mol), end-capping agents OEOacr and EPPETA, the intermediate product of the 1st step of the reaction PCL-IPDI and the final products UPCL-2 and UPCL-6.*

The number average molar mass (Mn) of PCL-IPDI (7200 g mol^{-1}) was found ≈2.3 times higher than the experimental Mn of the starting product PCLdiol (3100 g mol^{-1}). This is explained with the repetition of "PCL-IPDI" units in the synthesis of the precursors. The repetition effect in the precursors can be explained as follows. IPDI is a non-symmetrical diisocyanate that consists of a primary and a secondary isocyanate. During the urethanization reaction, the selectivity on the isocyanates of IPDI strongly depends on the temperature, catalyst type and orientation (i.e. *cis, trans*) of the substituents on the cyclohexane ring of IPDI. Although most organo-tin catalysts (e.g. DBTL) are selective over the secondary isocyanates, it has been reported that the selectivity of Bi-based catalysts is lower compared to its alternatives. [R1] A decreased selectivity of the catalyst results in the reaction of a certain amount of the primary isocyanate groups of IPDI as well as the secondary isocyanate groups in the 1st reaction step. This leads to the formation of repeating "PCL-IPDI" units, and hence, an increase in the molar mass, as evidenced in Figure S4.

Lower selectivity of the Bismuth based catalysts is not necessarily considered as a disadvantage for the target application. Although organo-tin catalysts provide a highly fast and selective reaction, they are highly toxic for almost all kind of cells. On the other hand, bismuth-based compounds are considered as a biocompatible alternatives as catalysts for various polymer syntheses. [R2] Indeed, our biocompatibility tests revealed no cytotoxic effect of the Bismuth neodecanoate at relevant concentration ranges.

The ≈2.3 times higher molar mass of PCL-IPDI compared to that of PCLdiol suggests that the repetition of PCL-IPDI (denoted as 'm' in Figure **S1**) equals to 2.3 on average. The UPCL-2 (9020 g mol^{-1}) final product had a similar molar mass distribution with the intermediate product PCL-

IPDI, suggesting that no other repetition effect occurred at the 2nd step of the reaction. The slightly higher molar mass of the UPCL-2 compared to that of PCL-IPDI is explained with the addition of the end-capping agent OEOacr at the 2nd reaction step.

In contrast, a remarkable shift was observed between the molar mass of PCL-IPDI and UPCL-6. This is explained with the presence of multiple hydroxyl groups in part of the EPPETA molecules, as the compound is a mixture of isomers. This resulted in the reaction of one end-capping agent with 2 or more PCL-IPDI units, resulting in a slightly increased molar mass with higher dispersity.

As a result of the repetition effect in both reactions, a fraction of low molar mass by-products or adducts are visible in the chromatograms of the final products (indicated with arrows in S 3). These are assigned to the adducts of "OEOacr-IPDI-OEOacr" and "EPPETA-IPDI-EPPETA" in UPCL-2 and UPCL-6 in a respective order, and the unreacted end-capping agents in the case of UPCL-6, that were most likely lacking hydroxyl groups.

5. Photo-rheology tests

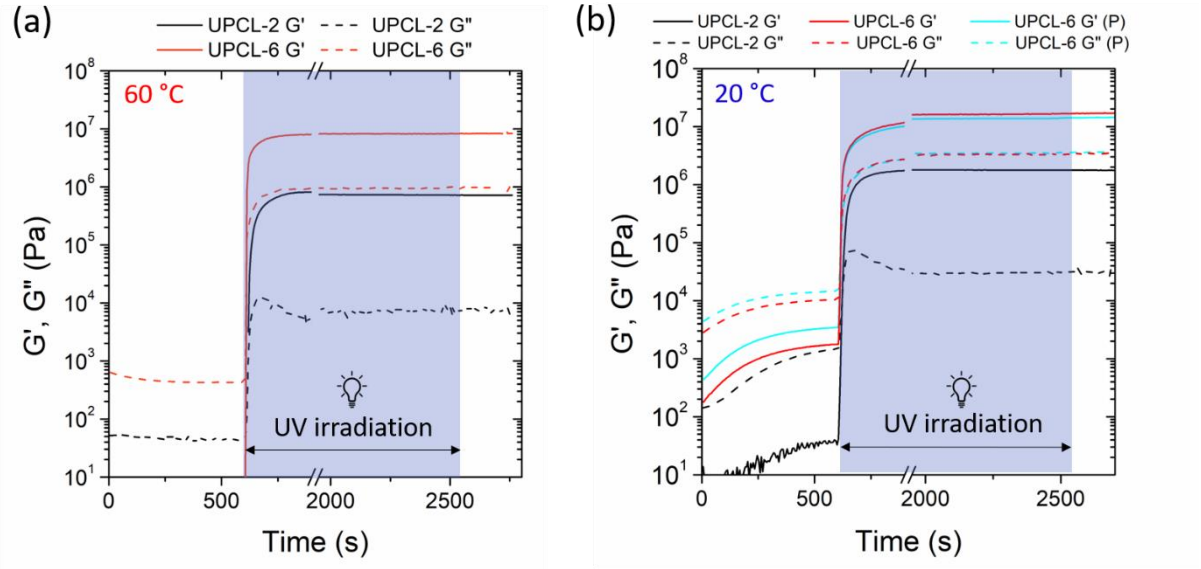

S5: *Storage and loss moduli of UPCL-2 and UPCL-6 recorded during photo-rheology experiments performed at (a) 60 °C and (b) 20 °C. (UPCL-6 (P) is referred to UPCL-6 that was initially purified via dialysis prior to the experiments.)*

The storage and loss moduli of the precursors before, during and after the curing process are presented in S5 for two different temperatures (20 °C and 60 °C).

For the samples that were tested at 60 °C, the loss moduli of both precursors were higher than the storage modulus prior to UV irradiation (0-600 s), confirming that they are in the liquid state **(S5 (a))**. Upon switching on the UV source, the moduli of both precursors showed a steep increase as a result of network formation. Shortly after the onset of UV exposure, the storage and loss moduli reached a plateau value indicating the completion of cross-linking. The crosslinked networks of UPCL-6 resulted in one order of magnitude higher storage modulus compared to that of UPCL-2.

For testing the moduli of the samples at 20 °C **(S5 (b))**, the precursors were initially molten at 60 °C for sample loading and subsequently cooled down to 20 °C before the start of the

measurements. The slight increase observed in storage and loss moduli over time prior to UV irradiation (0-600 s) can thus be explained with the start of physical interactions in the prepolymers (e.g. hydrogen bonding) at 20 °C. Nevertheless, the loss moduli of all samples remained higher than the storage moduli, indicating that the samples remained in the liquid state within this time frame (i.e. prior to UV irradiation). Both polymers remained highly reactive despite lower temperatures as evidenced via the steep increase at the start of UV irradiation.

As mentioned earlier, the products UPCL-2 and UPCL-6 were tested after synthesis without further purification. However, impurities present in the prepolymer UPCL-6 (e.g. unreacted end-capping agents, as evidenced in GPC analysis) may have an impact on the physical properties by acting as "crosslinkers". Herein, we also performed the photo-rheology experiments for the purified UPCL-6 (i.e. UPCL-6 (P)), in order to determine if the impurities in the prepolymer have an effect on the rheological properties. To this end, the UPCL-6 prepolymer was dialyzed for 3 days after dissolving in acetone (Spectrum™ Spectra/Por™ RC dialysis membrane, molecular weight cut off : 1 kDa), and subsequently dried under vacuum. After dialysis, acrylate concentration in the prepolymer UPCL-6 was reduced from 1.74 mmol g^{-1} to 1.53 mmol g^{-1} (determined via ^{1}H-NMR), which was associated with the removal of unreacted end-capping agents. Interestingly, removal of the unreacted end-capping agents and the reduction in acrylate concentration did not have a remarkable impact on the UV-induced crosslinking profile, as evidenced by the fairly similar moduli observed for UPCL-6 and UPCL-6 (P) during and after UV irradiation **(S5 (b))**. This result is indicating that, the impurities present in the UPCL-6 does not have a remarkable impact on the final physical properties.

6. Differential scanning calorimetry

Thermal properties of crosslinked UPCL-2 and UPCL-6 were determined using differential scanning calorimetry (DSC, TA instruments, Q2000 DSC). Samples (4-6 mg) were placed into Tzero aluminum DSC pans and subsequently sealed using an aluminum Tzero lid. The samples were then placed into the device furnace and equilibrated at 45 °C prior to the start of the analysis. An initial heating cycle was applied to remove the thermal history of the samples by heating up the precursors up to 100 °C at a controlled rate of 10 °C min^{-1}. Next, the precursors were cooled down to -80 °C at a controlled cooling rate of 5 °C min^{-1} and equilibrated at -80 °C for 10 minutes. Finally, the samples were heated again up to 100 °C at a controlled rate of 10 °C min^{-1}.

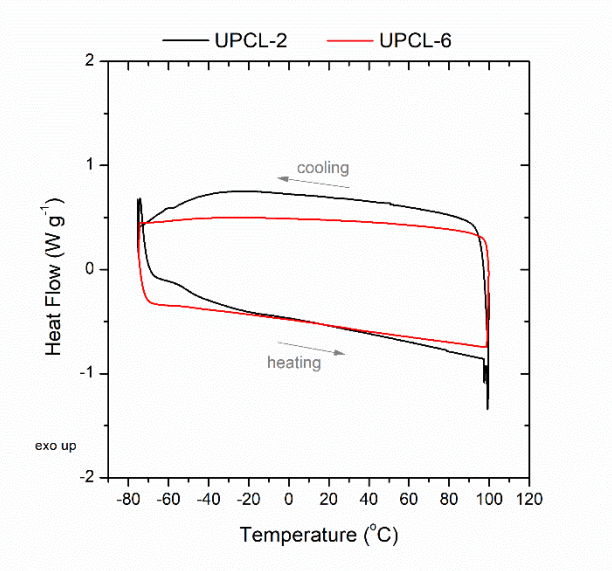

S6: Thermograms of crosslinked UPCL-2 and UPCL-6 as determined via DSC analysis

7. *In vitro* cytocompatibility tests

Morphologies of the L929 fibroblasts cultured in UPCL-6 extracts and control groups were monitored using an optical microscope (LSM 70, Zeiss, Germany) and the images are presented in S7.

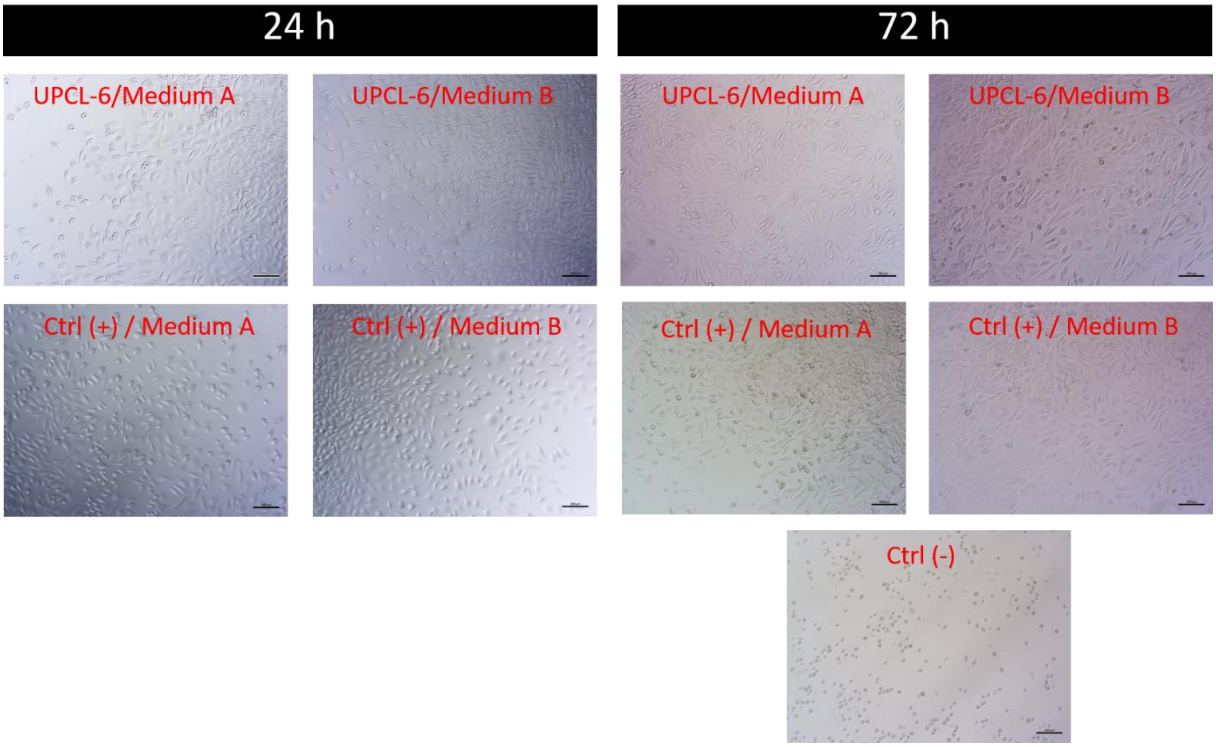

S7: *Optical microscopy images of the L929 fibroblasts cultured in UPCL-6 extracts, extract-free media (Ctrl (+)) and extract-free medium supplemented with 10% DMSO (Ctrl (-)) (scale bars: 100 µm)*

Morphologies of the L929 fibroblasts that were cultured in UPCL-6 extracts were similar to those cultured in the extract-free media (Ctrl (+)), whereas those cultured in the negative

control group medium (medium supplemented with 10% DMSO) resulted in round cell morphologies.

8. Thermogravimetric analysis

UPCL-6 prepolymer was tested via thermogravimetric analysis (Q50 TGA, TA Instruments) in order to determine whether or not the prepolymers are thermally stable in the applied temperature range during processing. To this end, samples (10 mg) were placed in a Pt sample pan and automatically loaded into the device furnace. The experiment was performed in N_2 atmosphere. The temperature was set at 35 °C, after which the temperature was ramped up to 750 °C at a heating rate of 10 °C min^{-1}. Data were analyzed using TA Instruments Universal Analysis software.

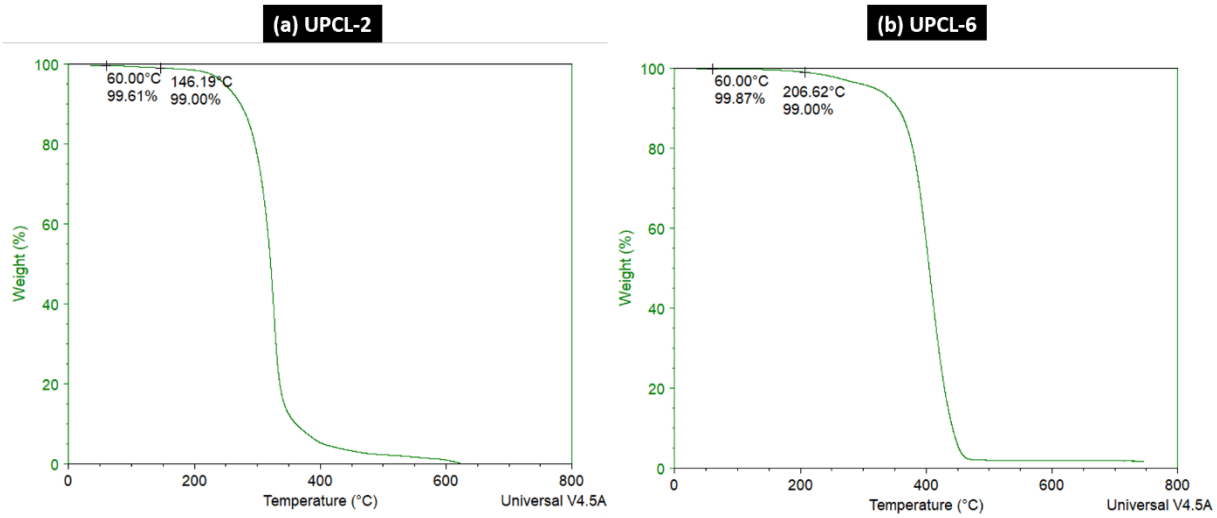

S8: *Thermograms obtained from the TGA analysis performed on (a) UPCL-2 and (b) UPCL-6 prepolymers*

According to the thermogravimetric analysis data presented in S8, the precursors were stable at the applied processing temperature range (mass loss < 0.40% up to 60 °C). The temperatures at which the prepolymers showed 1% mass loss were above 140 °C.

9. Water uptake capacity and hydrophilicity

Water uptake capacity and hydrophilicity of the crosslinked UPCL-2 and UPCL-6 were characterized via swelling and static contact angle tests, respectively.

For evaluation of the water uptake capacity, the crosslinked films (D: 6 mm, thickness: 1 mm) were initially weighed in dry state (Wd). Next, the samples were incubated in phosphate buffered saline (PBS) for 24 h at 37°C. At the end of incubation, the samples were removed from PBS, gently wiped with paper to remove excess water, and weighed (Ws). The water uptake capacity of the samples were calculated according to the following formula:

$$Water\ uptake\ capacity\ (\%) = \frac{Ws - Wd}{Wd} \text{ x } 100$$

Static contact angle values of the samples were obtained by the sessile drop method using an OCA 20 (DataPhysics Instrument GmbH, Filderstadt, Germany) device, and analysed with SCA 20 (DataPhysics Instrument GmbH, Filderstadt, Germany) software. After placing 1 µl deionized water onto crosslinked thin films, the drop was monitored via a micro camera and the contact angle was calculated via the circle fitting method. SCA values were recorded 60 seconds after the water contact.

The water uptake capacity and the static contact angle using water of a linear, non-crosslinked PCL thin film (Mn: 10,000 g mol^{-1}, Sigma-Aldrich) was tested at the same conditions as the control groups. For each test, triplicate samples were used.

The water uptake capacity and the static contact angle of the crosslinked samples are depicted in Figure S9. As anticipated, the water uptake capacity of the crosslinked UPCL-2 and UPCL-6 remained below 5% as a result of their hydrophobic nature. The low water uptake capacity is advantageous for preventing the micro-scaffolds against swelling-related deformations while incubating in cell culture medium.

As anticipated, a moderate wettability was observed for UPCL-6 films with an average water contact angle of 79.4° (S9). The water contact angles of both UPCL-2 and UPCL-6 networks were found to be significantly higher than that of linear PCL (68.4°), which can be attributed to the presence of hydrophobic polyacrylate chains present in the UPCL-2 and UPCL-6 networks.

It is well-known that PCL-based scaffolds lack cell-interactive properties due to their synthetic and hydrophobic structure. In order to overcome this limitation, various modification strategies have already been applied earlier on PCL-based scaffolds. In an earlier study of our group, hydrophilicity and cell-interactivity of PCL scaffolds were successfully improved via chemical surface modification techniques, such as plasma surface modification and covalent immobilization of gelatin [R3], which can be applied onto our newly developed polymers to increase their hydrophilicity and cell interactivity.

(a)

	PCL	UPCL-2	UPCL-6
Water uptake capacity (%)	0	4.1 ± 1.4	1.6 ± 1.3
Water contact angle (°)	68.4 ± 3.2	78.0 ± 2.4	79.4 ± 2.6

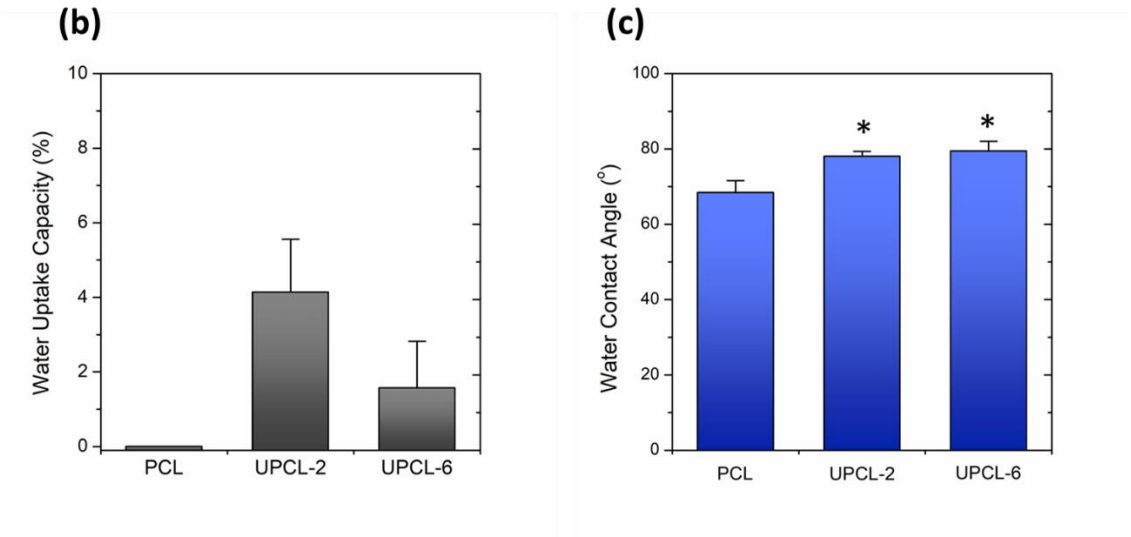

S9: *Water uptake capacity and water contact angle of samples (The statistical analysis was performed by one-way ANOVA with Tukey post-test, with * $p < 0.05$ in comparison with the PCL control group)*

10. Two photon polymerization

The initial working window for the materials was established by structuring cubes of 50 x 50 x 50 µm^3 (**S10**). The minimum required laser power was evaluated under direct light microscope. With M2CMK the threshold power significantly decreased from 60 to 10 mW compared to 4-4'-Bis (N,N-diethylamino) benzophenone.

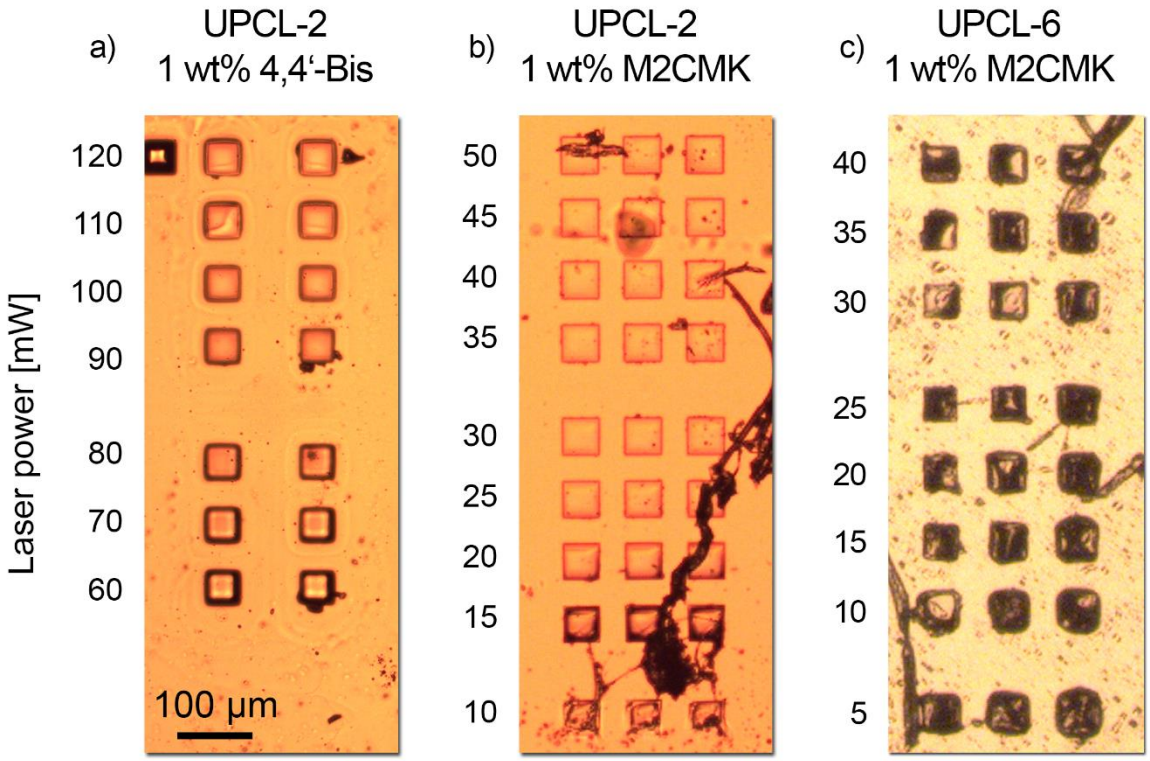

S10: *Polymerization threshold studies with UPCL-2. Cubes (50 × 50 × 50 µm^3) were structured with decreasing laser power (150 to 10mW). With 4,4'-Bis reduced the required power was above 40mW (left). With M2CMK it was possible to reduce the laser power down to 10 mW (right).*

While simple geometries such as cubes (**S10**) were possible to structure from UPCL-2, complex geometries such as the racecar depicted in **S11** already deformed during development. This effect was magnified after the solvent was evaporated. In contrast, the race car structured using UPCL-6 was stable after developing as shown in SEM image **(S12)**.

Nanoindentation measurements for 8 cubes printed using UPCL-6 are summarized in **S13**.

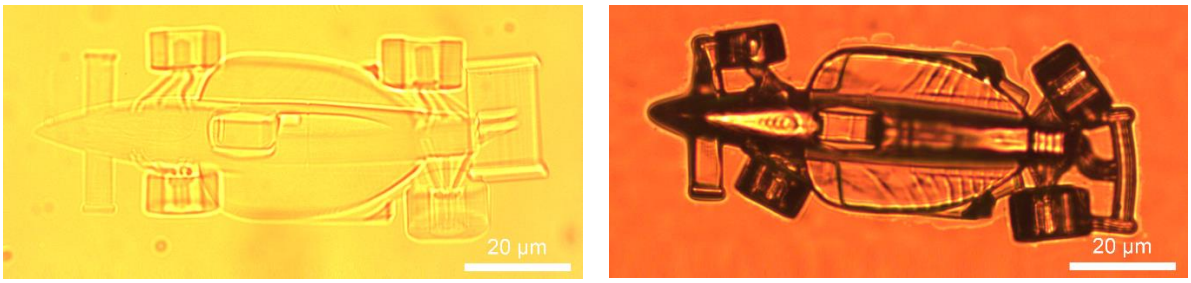

S11: *Race car structured with UPCL-2 (1 wt% M2CMK) using the 63x/1.4 objective. While the sample was developed in THF deformations could already be observed under the direct light (left). After the solvent evaporated the structure got deformed (right).*

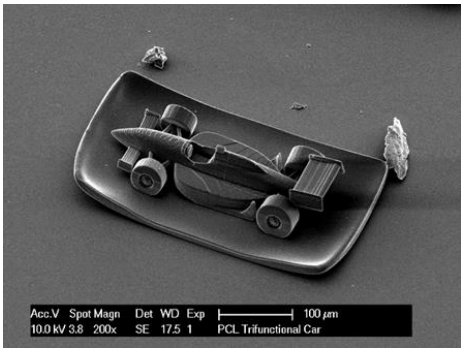

S12: *SEM image of the race car structured with UPCL-6*

S13: *Results for nanoindentation results for 2PP cubes fabricated from UPCL-6.*

Cube Nr.	Reduced Young's modulus [MPa]	Nr of Measurements
1	41.8 ± 12.4	7
2	34.4 ± 11.5	5
3	40.0 ±12.4	11
4	39.4 ± 9.5	9
5	39.0 ± 11.1	8
6	39.9 ± 9.2	12
7	39.6 ± 8.2	11
8	41.1 ± 8.4	11
Total	39.7 ± 9.8	74

References

[R1] R. Lomölder, F. Plogmann, and P. Speier. "Selectivity of isophorone diisocyanate in the urethane reaction influence of temperature, catalysis, and reaction partners." *Journal of Coatings Technology* **69**, 51-57 (1997).

[R2] H. R. Kricheldorf, ‘‘Syntheses of Biodegradable and Biocompatible Polymers by Means of Bismuth Catalysts.’’ *Chemical Reviews* **109**, 5579-5594 (2009).

[R3] T. Desmet, T. Billiet, E. Berneel, R. Cornelissen, D. Schaubroeck, E. Schacht, P. Dubruel, ‘‘Post-Plasma Grafting of AEMA as a Versatile Tool to Biofunctionalise Polyesters for Tissue Engineering’’, *Macromolecular Bioscience* **10**, 1484–1494 (2010).